Civil and Environmental Engineering
Vol. 21, Issue 2, 1402-1415, DOI: 10.2478/cee-2025-0102

PRELIMINARY VERIFICATION OF EXPERIMENTAL TESTS OF THE EXPLOSION RESISTANCE OF COMPOSITE STEEL-CONCRETE ELEMENTS MADE OF UHPFRC AND NSC

Adam ČÍTEK[1], David ČÍTEK[1], Vojtěch ŠULC[2], Marek FOGLAR[2], Radek HÁJEK[2], Karel HURTIG[1], Martin VAVRUŠ[3]

[1] Klokner Institute, CTU in Prague, Šolínova 7, 166 08 Prague, Czech Republic.
[2] CTU in Prague, Faculty of Civil Engineering, Thákurova 7, 166 29 Prague, Czech Republic.
[3] University of Zilina, Faculty of Civil Engineering, Univerzitná 8215, 010 26 Žilina, Slovakia.
[*] david.citek@cvut.cz

Abstract

Resistance of structures to blast effects currently represents one of the key topics in structural engineering. Explosions generate extreme dynamic localized loads that can cause severe damage or even failure of structures not specifically designed for such loading. Considering the outstanding mechanical performance and durability of ultra high-performance fibre reinforced concrete, as well as the favourable blast response of steel-concrete composite systems, the use of this modern cementitious material instead of conventional concrete in composite elements can significantly increase their blast resistance.
This paper presents an overview of a preparation of experimental program in which composite steel–concrete slabs and columns were manufactured and tested. Within the experimental program, steel elements, as well as composite elements with normal-strength concrete and ultra high-performance fibre reinforced concrete infill, were prepared and subjected to blast loading. The main objective was to evaluate the influence of the concrete material and the type of steel–concrete interaction on the overall blast resistance. The paper provides a detailed description of the specimen fabrication process, material properties of the applied concrete mixtures, experimental setup, and a concise discussion of the obtained results.

Keywords:

Concrete;
UHPFRC;
NSC;
Blast resistance;
Steel-concrete composite.

1 Introduction

Blast loading represents one of the most hazardous forms of dynamic action on civil engineering structures. While loads induced by wind or seismic activity can be modelled and predicted with reasonable accuracy, an explosion is characterized by an extremely rapid rise in pressure, short duration, and highly localized effect. The primary consequence is the formation of a shock wave that propagates through the surrounding medium and induces severe stresses in structures located near the explosion epicentre [1,2].

Historically, blast resistance was primarily associated with military facilities. However, in recent decades, the issue has become increasingly relevant in civil engineering as well, particularly in connection with the ongoing war in Ukraine, the threat of terrorist attacks, and accidental explosions in industrial facilities. Bridges, railway stations, office buildings, and critical infrastructure are all potentially exposed to blast hazards, and their reliability under such extreme events is essential for the protection of human life and property [3].

Normal-strength concrete (NSC), although one of the most widely used structural materials, exhibits significant brittleness under blast loading. When subjected to an explosion, NSC elements fail suddenly, accompanied by fragmentation and rapid loss of load-bearing capacity. If the energy generated by the explosion is sufficiently high, local perforation may occur together with spalling or scabbing on the rear face. The detached fragments can function as high-velocity projectiles, causing additional secondary damage. Similar behaviour and disadvantages can also be observed in purely steel structures [4,5].

Steel–concrete composite elements have attracted growing attention in recent years due to their superior structural efficiency and resilience under extreme loading conditions, including explosions and impact. Compared to elements made of a single material, such as plain concrete or steel, these composite systems exhibit markedly improved blast resistance resulting from the mutual interaction between steel and concrete. The steel shell provides ductility, confinement, and redistribution of the blast impulse, effectively preventing local perforations and reducing stress concentrations. The concrete infill, on the other hand, increases overall stiffness, attenuates the pressure wave, and stabilizes the steel section against local buckling or tearing. When sufficient composite action is ensured (typically by shear studs, laths, or other mechanical connectors) the two materials act together to share applied loads, enhancing global integrity, energy absorption capacity, and residual load-bearing resistance of the structure after a blast event [6,7,8].

A widely used example of such systems is the concrete-filled steel tube (CFST) column, in which the steel outer shell confines the concrete core, while the concrete prevents inward buckling of the steel wall. Previous research [7,9] demonstrated that concrete-filled steel members exhibit substantially higher strength and lower deformation under blast loading compared to hollow steel sections. However, most of these studies addressed far field or simplified blast scenarios. The behaviour of composite elements subjected to contact or near-field explosions, characterized by extremely high strain rates and steep pressure gradients, is still not fully understood. Under these conditions, stress concentrations can develop at the steel-concrete interface, potentially leading to partial delamination and loss of composite action. This phenomenon can significantly influence the internal propagation of blast waves and, consequently, the global failure mechanism of the structure, yet has not been thoroughly quantified.

Replacing normal-strength concrete with ultra-high-performance fibre-reinforced concrete (UHPFRC) offers a promising pathway to mitigate these issues and further enhance the blast resistance of composite systems. UHPFRC is a modern cementitious composite distinguished by its exceptional mechanical properties and durability, including compressive strengths of 150 - 200 MPa, high elastic modulus, and the ability to sustain tensile stresses after cracking owing to uniformly dispersed steel fibres [9,10,11]. These characteristics enable UHPFRC to limit crack initiation and propagation, maintain interfacial bond strength, and reduce delamination even under extreme dynamic loading.

The present research aims to experimentally verify the blast resistance of composite steel-concrete elements made of NSC and UHPFRC under contact detonation, with particular attention to the effects of interface behaviour and composite action. Unlike most previous studies that focused on isolated components or far field loading, this work investigates structurally relevant configurations such as slabs and columns, which are typical for real engineering applications. The obtained experimental data will serve as a basis for advanced numerical modelling and for the development of improved design recommendations for next-generation blast-resistant composite systems.

By integrating UHPFRC into steel-concrete composites, it becomes possible to define local energy dissipation zones through controlled material heterogeneity, thus enhancing structural robustness and reducing fragment projection. The combination of high-performance materials and efficient composite action represents a significant step forward in the design of protective structures exposed to extreme dynamic loads.

This paper summarizes the results of an experimental program carried out at the Faculty of Civil Engineering of CTU and Klokner Institute, focused on the development, fabrication, and testing of composite steel-concrete slabs and columns subjected to blast loading. The program aimed to compare the behaviour of pure steel, normal-strength concrete, and UHPFRC composite elements in terms of their structural response and damage mechanisms under explosive loading, and to quantify the effect of the composite material's inner structure on the propagation of blast loading through the material. This understanding is intended to be incorporated into the assessment of steel–concrete columns subjected to axial force, enabling more accurate evaluation of their structural response and residual load-bearing capacity under extreme dynamic conditions.

2 Description of test specimens and their fabrication

The experimental program was divided into two main parts, focusing on slab elements and column elements. Within each part, the design of the test specimens and the supporting numerical analyses were carried out at the Faculty of Civil Engineering, Czech Technical University in Prague (CTU), which served as the lead institution of the research project. The design phase included the development of specimen geometry, reinforcement detailing, and shear connection arrangements to ensure representative structural behaviour under blast loading. All specimens were designed and prepared in accordance with relevant Eurocode standards to ensure compliance with established structural design principles. The optimization of concrete mixtures, material properties tests, and fabrication of the experimental specimens were performed by the Klokner Institute (KI).

The slab specimens represented thin plate-type members primarily subjected to local impulsive effects, whereas the column specimens simulated vertical load-bearing components exposed to combined axial and blast-induced loading. The following section provides a detailed description of the geometry, materials, and fabrication procedures of all tested specimens.

2.1 Slab specimens

The first part of the experimental program focused on slab specimens. This part had two primary objectives – to compare the behaviour of several types of steel–concrete composite connections in slabs subjected to blast loading, and to evaluate the differences in structural response between normal-strength concrete (NSC) and UHPFRC. Test specimens were designed as square panels with dimensions of 1.0x1.0x0.15 m. The size was selected to allow the installation of standard reinforcement and shear connectors while maintaining manageable dimensions for laboratory handling. Before the fabrication of the test specimens, a simplified numerical analysis was carried out to predict the structural response under blast loading and to minimise potential adverse effects related to specimen size and experimental setup.

A total of twelve slab specimens were prepared, divided into two series according to the type of concrete used – Series 1 (NSC) and Series 2 (UHPFRC). Each series consisted of six variants differing in reinforcement arrangement and type of steel–concrete connection. Specimens 1.0 and 2.0 were reinforced with a welded reinforcement mesh Ø8/150/150 with a 30 mm concrete cover. Specimens 1.1 and 2.1 consisted of plain concrete with a bottom steel plate connected by four shear studs Ø10/100 placed in the corners. Specimens 1.2 and 2.2 were plain concrete slabs sandwiched between two 10 mm thick steel plates connected by four M10 threaded bars located in the corners, while specimens 1.3 and 2.3 had the same configuration but with twenty-four M10 bars to provide full connection. Specimens 1.4 and 2.4 consisted of concrete slabs with a bottom steel plate connected by twenty-four shear studs Ø10/100 to ensure composite action, additionally reinforced with a welded mesh Ø8/150/150 positioned at mid-depth. Finally, specimens 1.5 and 2.5 incorporated a bottom steel plate connected by six 5 mm thick shear plates to ensure composite action, with an additional welded reinforcement mesh Ø8/150/150 placed at the mid-height of the cross-section. The described specimen configurations are illustrated in Figures 1 and 2.

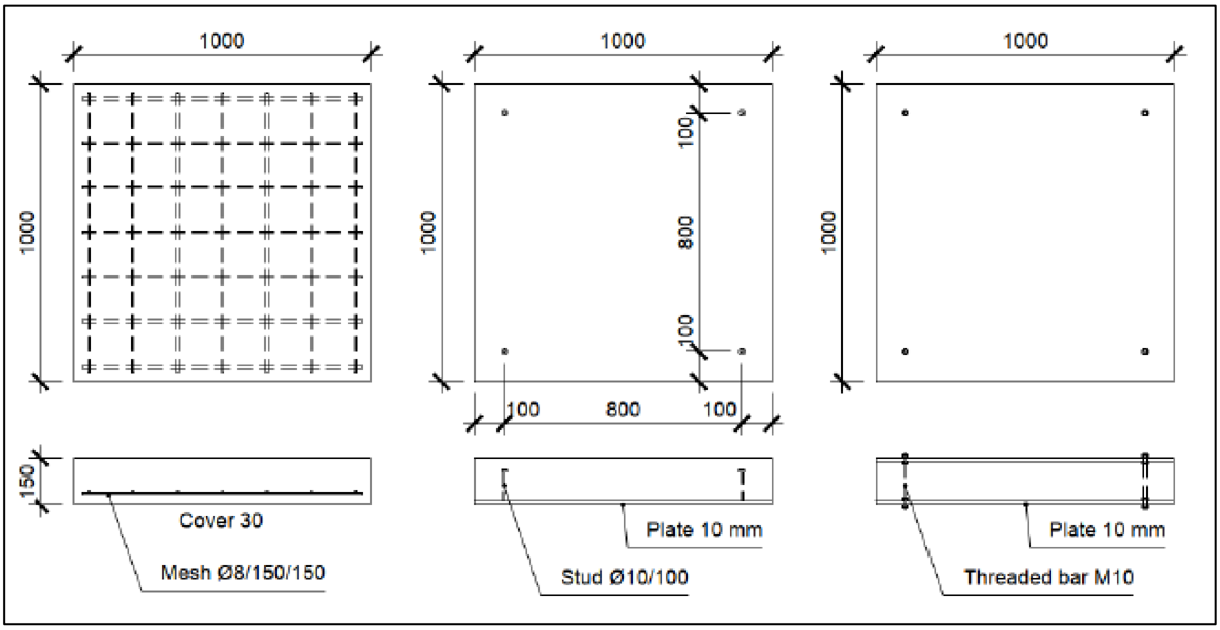

Fig. 1: Configuration of steel-concrete composite slabs – series 1.0–1.2 and 2.0–2.2.

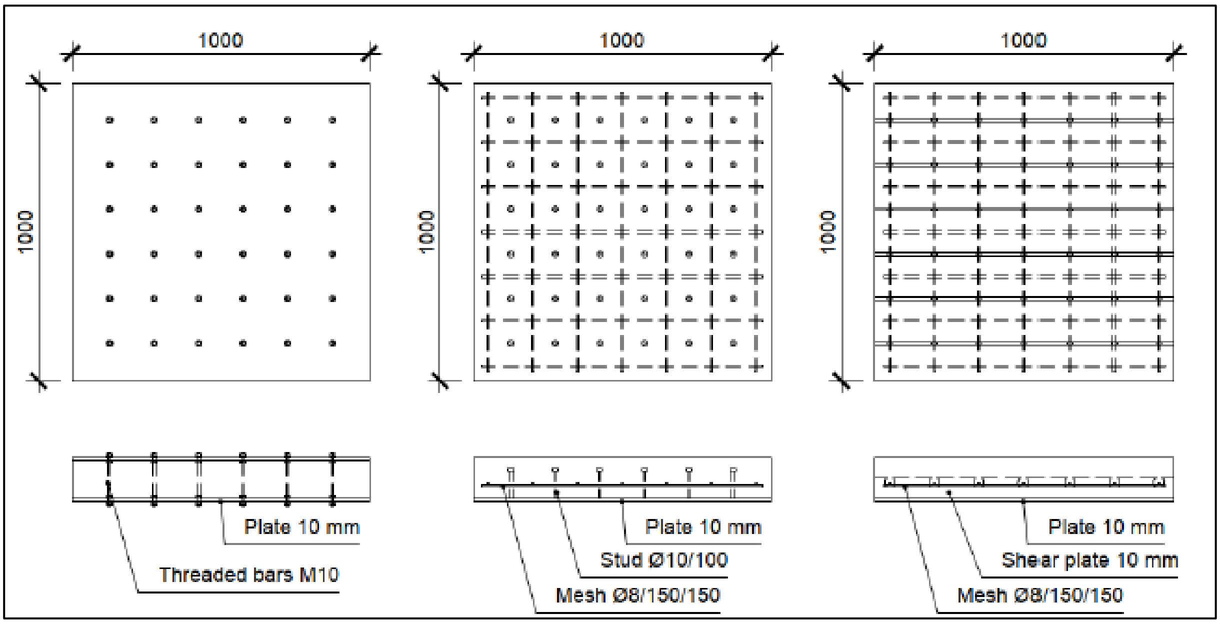

Fig. 2: Configuration of steel-concrete composite slabs – series 1.3–1.5 and 2.3–2.5.

After completing the specimen design and preliminary numerical analyses, the formwork system was designed and manufactured. Since the specimens were cast in a vertical position, the formwork had to be sufficiently stiff to resist the hydrostatic pressure of fresh concrete. The main formwork structure was made of 22 mm thick wooden boards reinforced with timber beams and connecting hardware. Steel plates, reinforcement meshes, and shear connectors were positioned inside the formwork and securely fixed from both sides prior to casting.

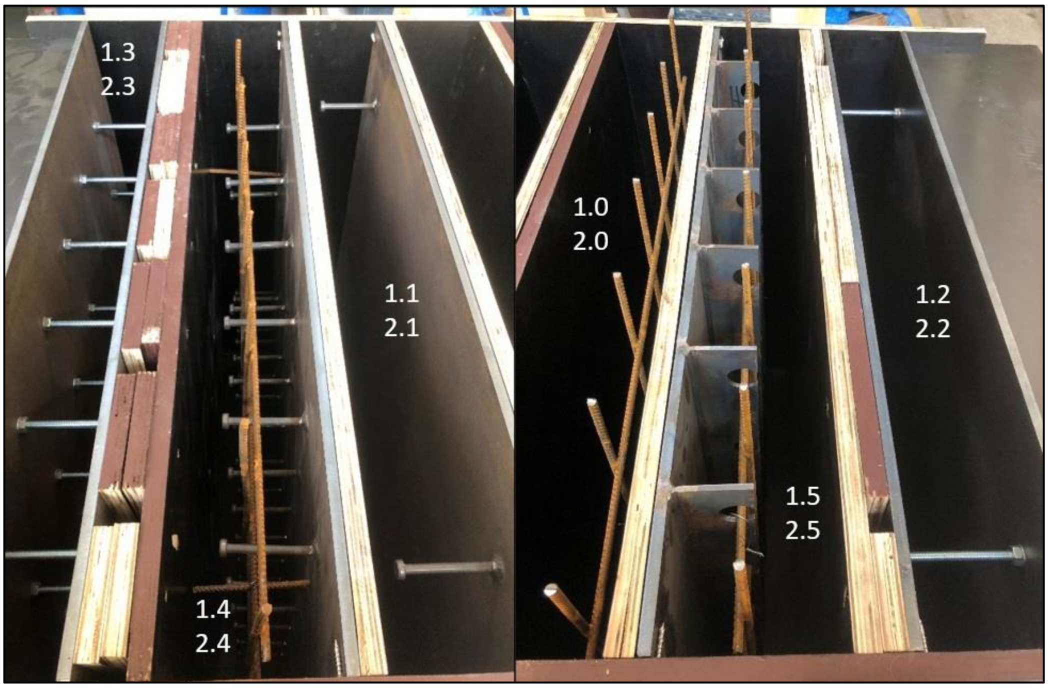

Fig. 3: Formwork arrangement for the casting of slab specimens.

The casting process was divided into two consecutive days. For normal-strength concrete (NSC) specimens, one batch of concrete was prepared at a concrete plant and delivered by a truck mixer. The NSC mixture was compacted using an immersion vibrator to ensure proper consolidation. In contrast, UHPFRC specimens were mixed from six individual batches with a total volume of approximately 0.9 m³. All dry constituents were pre-mixed and bagged in advance, which significantly accelerated the preparation and casting process. Due to the self-compacting nature of UHPFRC, no vibration was required during casting.At the final stage of casting, handling inserts were placed into the top surface to facilitate subsequent manipulation. After pouring, the exposed surface was treated with a curing compound and covered with plastic foil to prevent moisture loss. During the following days, the specimens were water-cured by spraying, ensuring proper hydration. After approximately one week, the formwork was disassembled, and the slabs were demoulded. No visible defects such as voids, cracks, or surface irregularities were observed. The completed specimens were after 28 days transported to the University of Pardubice, where the blast resistance tests were conducted. During both casting procedures, companion test specimens were also prepared to determine the mechanical properties of the concrete mixtures, and the results of these material tests are summarised in Chapter 3.

2.2 Column specimens

While the slab specimens represented plate-type members primarily subjected to local impulsive effects, the column specimens were designed to simulate vertical load-bearing elements exposed to a combination of axial compression and blast-induced loading. In total, ten column specimens were designed and fabricated, divided into three categories. Type 1 consisted of plain steel columns without concrete infill, serving as reference specimens. Type 2 represented composite steel–concrete columns filled with normal-strength concrete (NSC) and Type 3 comprised composite columns filled with UHPFRC.

All specimens were manufactured from hot-rolled HEA 220 steel profiles made of structural steel grade S355. Both ends of each profile were sealed with steel end plates to ensure uniform load transfer and maintain overall integrity during testing. To enable safe handling and accurate alignment during the experiments, auxiliary side plates were attached to the columns; these served purely as support fixtures and had no structural contribution to the specimen behaviour. The composite interaction between the steel section and the concrete core was achieved through shear connectors in the form of bent reinforcing bars welded to the inner web and flanges of the steel section.

To replicate realistic boundary conditions, spherical steel joints were installed at both ends of each column, providing pinned support conditions that allowed free rotation and ensured uniform axial load distribution across the section. These joints also enabled consistent boundary representation for subsequent numerical simulations. The schematic layout of the column specimen, including the longitudinal view and cross-section, is shown in Figure 4.

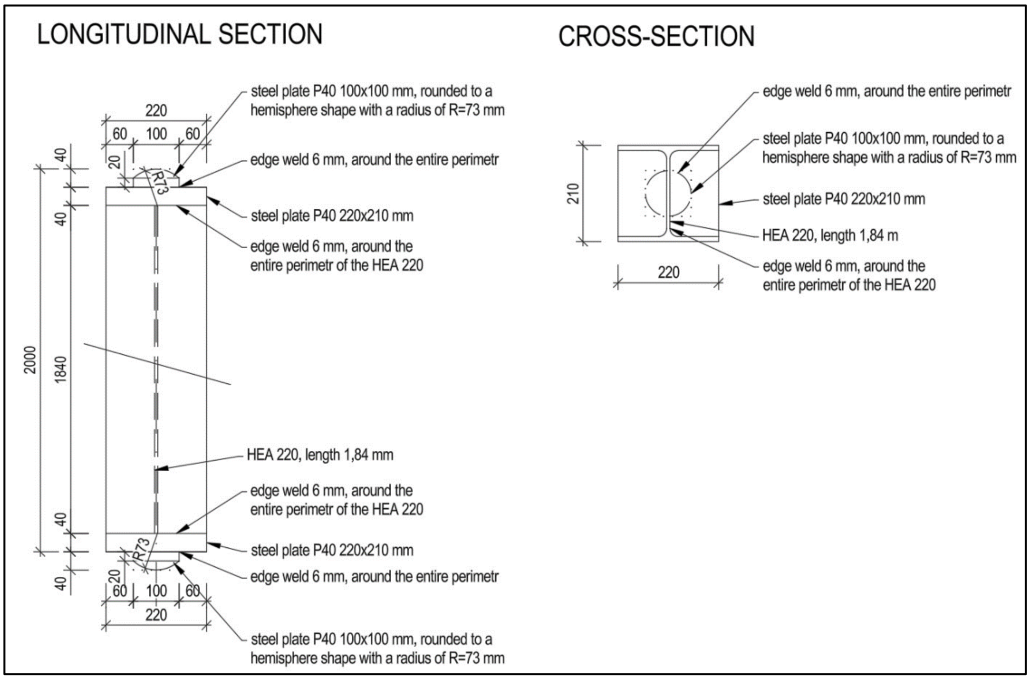

Fig. 4: Detailed description of the steel parts of the specimens in longitudinal section and cross-section.

The infill of columns was cast in a horizontal position, with the flanges oriented upwards. This arrangement allowed the steel section itself to serve as permanent formwork, eliminating the need for additional mould preparation. Since only one side of the column cross-section could be filled at a time, the casting procedure was divided into two phases. After the first side was cast, a two-day technological pause was maintained to allow sufficient setting of the concrete. Subsequently, the specimens were rotated around their longitudinal axis, and the second phase of casting was completed.

For the NSC specimens, the concrete was compacted using an immersion vibrator to ensure adequate consolidation and eliminate air voids. In contrast, the UHPFRC specimens did not require mechanical vibration due to the self-compacting nature of the mixture. Both concrete types were mixed and cast directly in the KI laboratories — the UHPFRC columns were produced in two batches with a total volume of approximately 0.45 m³, and the NSC columns in two batches totalling 0.5 m³.

Immediately after casting, the exposed concrete surfaces were treated with an evaporation retardant and covered with plastic foil to prevent rapid moisture loss. During the first two days, the surfaces were water-cured by spraying to promote proper hydration. After 28 days of curing, all column specimens were transported to the University of Pardubice, where the blast resistance tests were subsequently performed.

During both casting procedures, companion test specimens were also prepared to determine the mechanical properties of the concrete mixtures, and the results of these material tests are summarised in Chapter 3.

Fig. 5: Prepared steel columns with welded shear connectors prior to concrete infill casting.

Fig. 6: Composite steel–concrete columns after casting of the concrete infill.

3 Material properties

One of the primary objectives of the research project was to compare the mechanical behaviour of normal-strength concrete (NSC) and ultra-high-performance fibre-reinforced concrete (UHPFRC) used in the composite elements. This chapter presents the basic mechanical properties of the concrete mixtures employed in the experimental program. The material properties were determined through tests performed on companion specimens that were cast simultaneously with the slab and column specimens. These tests provided the necessary reference data for evaluating the performance differences between the two concrete types and for subsequent numerical modelling.

3.1 Normal strength concrete (NSC)

For the slab specimens, a ready-mix concrete of class C 30/37 XF2 S4 Dmax 16, CEM I 42.5 R, Cl 0.2 with a water–cement ratio of 0.45 was used. This mixture specification was selected based on previous experimental experience and ensured the required balance between mechanical strength and workability. Since the slabs were cast in a vertical position, sufficient flowability of fresh concrete was essential; therefore, a consistency class S4 and a maximum aggregate size of 16 mm were specified. The concrete was supplied from a ready-mix concrete plant and delivered to the Klokner Institute by a truck mixer, where the casting of the slab specimens was performed.

In contrast, the NSC used for the column specimens was mixed directly in the laboratory of the Klokner Institute. Due to different mixing and curing conditions, as well as variations in aggregate grading and compaction method, the resulting mechanical properties differed significantly from those of the concrete used for the slabs. The fundamental material properties of the NSC mixture at 28 days of age are summarised in the following tables 1 and 2.

Table 1: Material properties of NSC.

Mix ID	Material temperature [°C]	Slump test [mm]	Bulk density [kg/m3]	Average speed of UZ signal [km/s]		Modulus of elasticity
				beam 150x150x700 mm	cylinder 150/300 mm	cylinder 150/300 mm [GPa]
N1 (slabs)	26.4	100	2360	4.51	4.60	33.3
N2 (columns)	22.1	100	2370	4.57	4.53	33.0
N3 (columns)	22.3	110	2360	4.55	4.54	33.1

Table 2: Flexural and compressive strength of NSC.

Mix ID	Flexural strength	Compressive strength [MPa]			
	beam 150x150x700 mm [MPa]	cube 100 mm	cube150 mm	cylinder 100/200 mm	cylinder 150/300 mm
N1 (slabs)	3.41	48.1	43.9	39.4	36.5
N2 (columns)	4.03	60.7	55.4	52.3	49.5
N3 (columns)	3.95	59.1	50.2	50.2	47.3

3.2 Ultra-high performance fibre reinforced concrete (UHPFRC)

For the ultra-high-performance fibre-reinforced concrete, a mixture developed at the Klokner Institute was used, which was based on previous experimental experience and further modified specifically for the purposes of this project. The mixture was characterised by a very low water–cement ratio, self-compacting behaviour, and exceptionally high mechanical properties, including compressive and flexural strength as well as a high modulus of elasticity. The mixture was reinforced with 1.5% by volume of short steel fibres, uniformly dispersed within the cementitious matrix. This fibre dosage was selected as an optimal balance between mechanical performance (particularly flexural tensile strength and residual strength) and sufficient workability to ensure proper casting and complete filling of the composite joints and connection details.

The UHPFRC was produced entirely in the laboratory environment of the Klokner Institute, under controlled mixing and curing conditions to ensure homogeneity and repeatability. The key material properties of both the fresh and hardened UHPFRC mixtures at 28 days of age are summarised in the following tables 3 to 5. In addition to the standard mechanical characteristics, the ultrasonic pulse velocity was also measured to evaluate the propagation of stress waves through the material. Since the casting was carried out over two consecutive days, two sets of test results are presented to account for potential differences between batches.

Table 3: Material properties of UHPFRC.

Mix ID	Material temperature [°C]	Flow test [mm]	Bulk density [kg/m3]	Average speed of UZ signal [km/s]		Modulus of elasticity
				beam 150x150x700 mm	cylinder 150/300 mm	cylinder 150/300 mm [GPa]
U1 (slabs)	25.8	285x310	2420	4.66	4.61	44.9
U2 (columns)	25.0	285x290	2430	4.64	4.62	44.9
U3 (columns)	28.3	240x245	2410	4.61	4.58	44.7

Table 4: Compressive and flexural strength of UHPFRC.

Mix ID	Compressive strength [MPa]				Flexural strength [MPa]	
	beam 40x40x160 mm	cube 100 mm	cylinder 100/200 mm	cylinder 150/300 mm	beam 40x40x160 mm	beam 150x150x700 mm
U1 (slabs)	176.3	146.4	132.2	131.9	37.3	17.3
U2 (columns)	176.5	144.3	132.4	129.8	33.3	13.5
U3 (columns)	152.0	134.3	131.2	122.0	29.1	11.7

Table 5: Direct tensile and flexural strength of UHPFRC.

Mix ID	Flexural tensile strength at crack initiation [MPa]	Residual flexural strength for deflection of: [MPa]			Direct tensile strength at crack initiation [MPa]	Residual direct tensile strength for deflection of: [MPa]	
		0.5 mm	3.5 mm	5.0 mm		0.5 mm	3.5 mm
U1 (slabs)	13.5	14.6	12.2	9.0	9.3	6.8	4.4
U2 (columns)	11.2	12.6	11.7	9.1	8.5	6.4	4.3
U3 (columns)	9.6	11.5	10.5	9.1	5.8	5.8	3.8

4 Experimental tests

The experimental part of the research was conducted at the Institute of Energetic Materials of the University of Pardubice, where all blast tests were performed under controlled conditions. The specimens were installed on steel testing frames described in the following text. All experiments were carried out under identical blast loading conditions to ensure comparability of the results. The applied explosive charge consisted of 0.5 kg or 0.8 kg of Semtex 1A, depending on the specimen type, and was placed in direct contact with the surface of each tested element.

The displacement response of the specimens during the blast was measured using a four-channel Photonic Doppler Velocimetry (PDV) system, which recorded the time history of deflection at selected points. The obtained velocity and displacement data provided a basis for further numerical and analytical evaluation. After each blast test, the specimens were subjected to visual inspection, documenting all visible damage such as spalling, local perforations, and crack development in the concrete or steel components.

4.1 Slab specimens

The blast testing of the slab specimens was focused on evaluating the local and global response of the composite panels subjected to direct explosive loading. Each slab was positioned horizontally on a steel supporting frame, allowing free deformation of the soffit while maintaining stable boundary conditions. The explosive charge of 0.5 kg Semtex 1A was placed at the centre of the top surface of each specimen, ensuring consistent loading conditions across all configurations.

During the tests, the dynamic response of the slab soffit was recorded using four PDV channels, measuring displacement time histories with high temporal resolution. These data provided crucial information for comparing the behaviour of NSC, UHPFRC, and pure steel specimens, as well as for calibration of subsequent numerical simulations. After detonation, each specimen was carefully examined, and the extent of cracking, spalling, and potential perforation was documented on both the top and bottom surfaces. The test setup is illustrated in Figure 9.

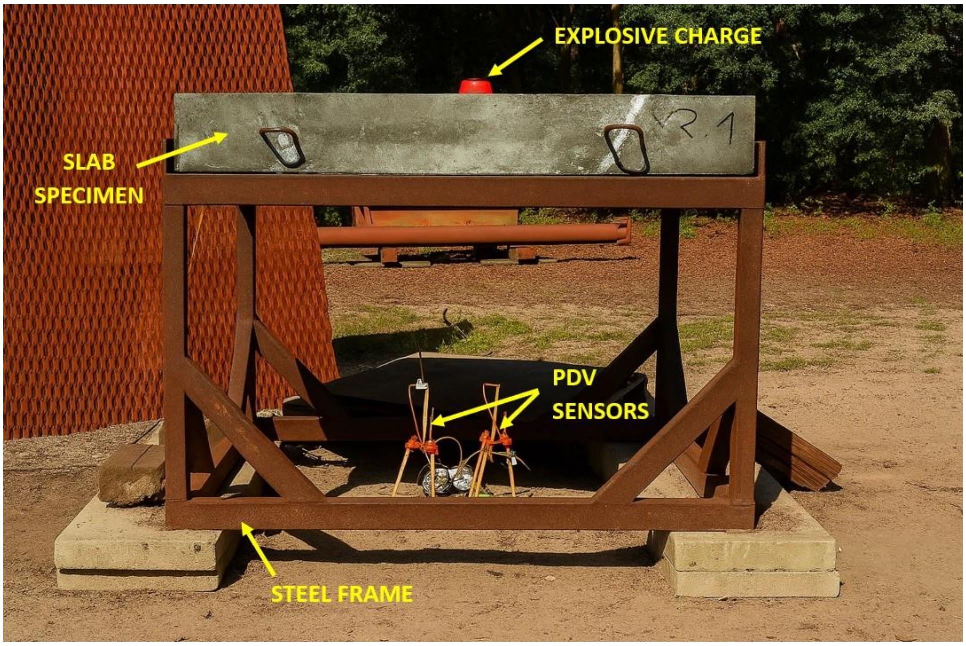

Fig. 9: Test set-up for blast tests of slab specimens.

4.2 Column specimens

The column tests were designed to simulate the combined effect of axial compression and blast loading acting on vertical load-bearing members. For this purpose, a specialized testing apparatus was developed to ensure sufficient stiffness, durability, and safety during the experiments. The test frame was designed as a statically indeterminate steel structure, providing prestressing through a hydraulic jack located at the base. This arrangement allowed controlled application of the axial compressive load while avoiding unintended bending effects. The hydraulic jack and supporting parts were enclosed in a protective steel housing to prevent damage during detonation. The final setup of the testing apparatus is shown in Figure 10.

Prior to each test, the column specimens were placed vertically in the loading frame, and an axial compressive load corresponding to the typical corner column loading of a multi-storey building was applied – either 100 kN for reference tests or 1,300 kN for full-scale simulations. The blast charge, consisting of 0.8 kg of Semtex 1A, was moulded into a rectangular shape and placed in direct contact with the outer flange of the steel section at mid-height. The dynamic response of the specimens was recorded using the same PDV system, while additional strain gauges mounted on the frame columns monitored axial forces and residual load capacity after the blast. The strain gauges were installed on the outer sides of both vertical columns of the steel frame to minimize the risk of damage caused by the blast-induced shock wave, as can be seen in Figures 10 and 11.

Fig. 10: Steel testing frame with the mounted column specimen before the blast test.

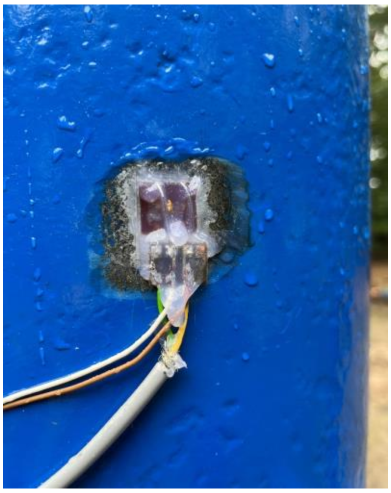

Fig.11: Placement of strain gauges along the side of the steel testing frame.

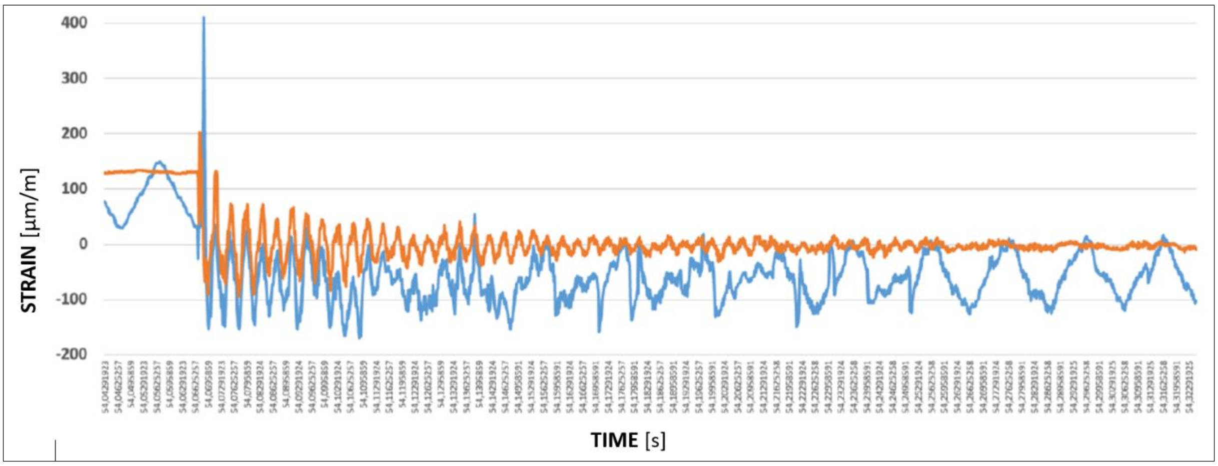

Fig. 12: Example of strain measurements on the steel frame during the blast loading.

5 Results

The results presented in this chapter briefly summarise the findings of the blast resistance experiments performed on both slab and column specimens. The experimental program was aimed at evaluating the influence of the material type and the effectiveness of composite interaction between steel and concrete components. The evaluation focused primarily on observed damage patterns and qualitative assessment of the specimens' dynamic response. Measured displacement time histories and visual documentation form the basis for a more detailed analysis, which is currently in progress.

All specimens were visually examined after the detonation, and the typical damage patterns were compared across material types and structural configurations. The observations, supported by Photonic Doppler Velocimetry (PDV) measurements, provide an initial insight into the global and local response mechanisms of the tested elements under extreme loading conditions. A more detailed evaluation of the experimental data, including the analysis of PDV sensor outputs, is currently underway as part of the ongoing research.

5.1 Slab specimens

The blast tests on slab specimens revealed a marked improvement in resistance and integrity for elements made of UHPFRC compared to those made of NSC. Specimens from UHPFRC generally exhibited significantly lower levels of visible damage, confirming the material's superior performance under high-intensity impulsive loads.

This was evident particularly in the reference specimens 1.0 and 2.0, composed solely of concrete and conventional reinforcement. The NSC specimen suffered severe damage and loss of integrity, while the UHPFRC specimen displayed only a localized impact crater on the upper surface caused by pressure-induced spalling. Similar results were recorded for specimens 1.1 and 2.1, which incorporated a steel plate on the soffit. The NSC version was completely breached, while its UHPFRC counterpart maintained its overall integrity with only a shallow crater and minor spalling in the impact zone.

The results also confirmed the positive influence of effective composite action between steel and concrete. In specimens where shear connectors were used more extensively (e.g., 24 connectors in specimens 1.4 and 2.4 compared to 4 in specimens 1.1 and 2.1), the overall damage was substantially reduced. Specimens 1.4 and 2.4 showed no visible damage on the soffit and only small craters on the top surface. UHPFRC versions of these configurations displayed even smaller and more localized damage.

In cases where the slabs were sandwiched between two steel plates (specimens 1.2, 1.3, 2.2, and 2.3), the observed damage was limited to local puncturing of the upper plate, while no failure or visible deformation appeared on the lower surface. The differences in failure patterns between the NSC and UHPFRC specimens are illustrated in Figures 12 to 19.


Fig. 12: Topside of specimen No. 1.0.

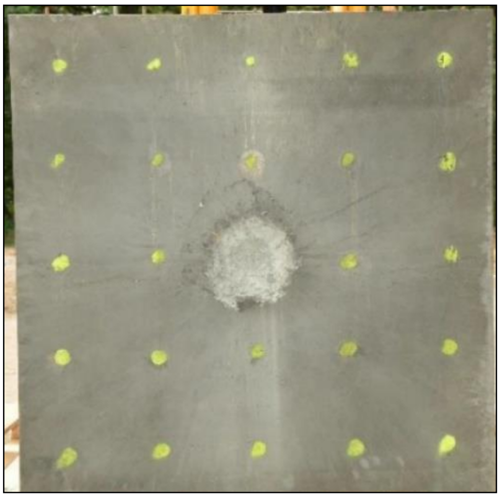
Fig. 13: Topside of specimen No. 2.0.


Fig. 14: Topside of specimen No. 1.1.

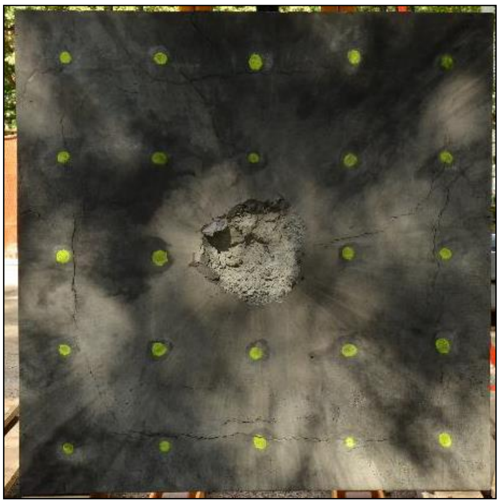
Fig. 15: Topside of specimen No. 2.1.


Fig. 16: Topside of specimen No. 1.4.

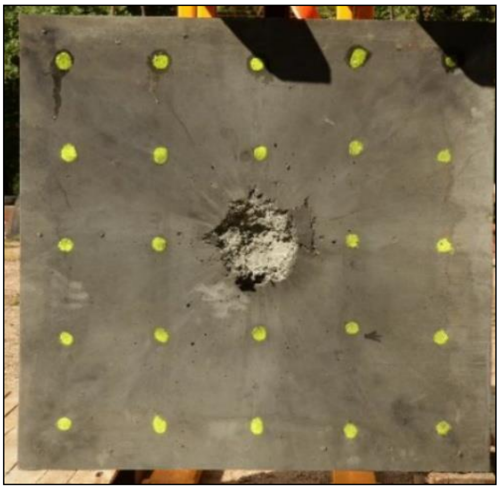
Fig. 17: Topside of specimen No. 2.4.

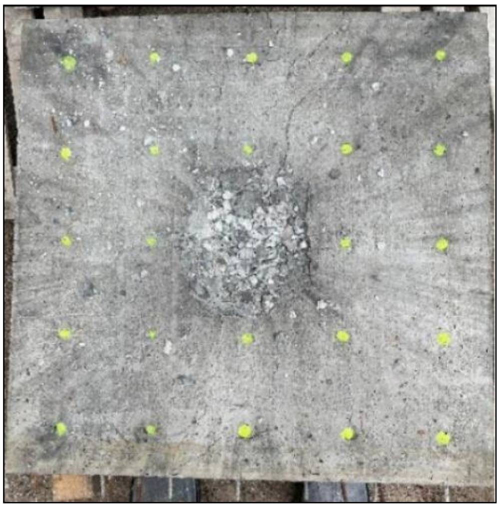

Fig. 18: Topside of specimen No. 1.5.

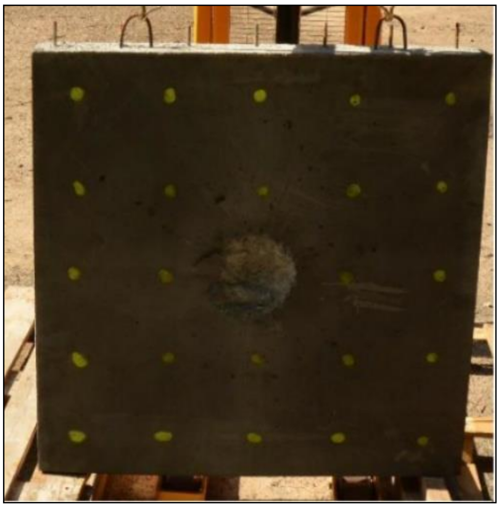

Fig. 19: Topside of specimen No. 2.5.

5.2 Column specimens

The column tests confirmed the beneficial effect of concrete infill on the blast resistance of steel sections. Hollow steel columns (Type 1) showed extensive local damage, including tearing and detachment of flange fragments on the side directly exposed to the explosion. Detached fragments also impacted the opposite flange, leading to secondary damage.

Fig. 20: Side view of only steel specimen (type 1).

The composite columns (Types 2 and 3) filled with concrete exhibited significantly reduced damage. The concrete infill effectively prevented fragmentation of the steel flange in contact with the explosive and absorbed part of the blast energy through localized crushing and spalling near the impact area. The opposite flanges of these specimens remained largely intact, demonstrating the protective function of the concrete core.

When comparing NSC and UHPFRC-filled columns, the difference in residual condition was pronounced. NSC-filled columns displayed deeper spalling and more extensive crushing, while UHPFRC-filled columns retained their shape with only minor surface cracking and no significant delamination between the steel and concrete components. The superior cohesion and strength of UHPFRC contributed to better energy dissipation and reduced deformation of the steel shell under blast loading.

Fig. 21: Side view of composite specimen with NSC infill (type 2).

Fig. 22: Side view of composite specimen with UHPFRC infill (type 3).

6 Conclusion

The experimental program presented in this paper focused on the evaluation of blast resistance of composite steel–concrete elements made of normal-strength concrete (NSC) and ultra-high-performance fibre-reinforced concrete (UHPFRC). Both slab and column specimens were subjected to controlled explosive loading to assess the influence of material type, degree of composite interaction, and overall structural configuration on the observed response.

The results clearly demonstrated the superior blast performance of UHPFRC compared to conventional NSC. Specimens incorporating UHPFRC exhibited reduced spalling, smaller crater formation, and improved structural integrity after detonation. Furthermore, a strong composite connection between the steel and concrete components proved to be a key factor in achieving enhanced resistance, as it allowed efficient load transfer and minimized local damage. In column specimens, the presence of concrete infill substantially increased the structural robustness of the steel section, with UHPFRC-filled columns showing the lowest deformation and least visible damage among all tested configurations.

Overall, the experimental observations confirmed that the use of UHPFRC in steel–concrete composite systems can significantly extend their performance limits under extreme dynamic loading, providing higher safety margins and improved residual capacity after a blast event.

A detailed analytical and numerical evaluation of the recorded data, including displacement histories, strain measurements, and post-blast residual strength, is currently ongoing. The findings from this subsequent analysis will be used to develop validated numerical models and design recommendations for the application of UHPFRC in protective and load-bearing structures exposed to blast effects.

Acknowledgement

The article was written with the support of the grant project of the Czech Science Foundation – project No. 22-33039S.

References

[1] CORMIE, D. - MAYS, G. - SMITH, P.D.: Blast effects on buildings. Thomas Telford Publishing, 2009.
[2] ALAWAD, O. M.: Assessment of a Simplified Methodology for Preliminary Blast-Resistant Design of Insulated Precast Concrete Wall Panels. Civil and Environmental Engineering, Vol. 20, Iss. 1, 2024, pp. 41–53, doi: 10.2478/cee-2024-0004.
[3] PARK, S. - SCHLEYER, G.K.: Concrete behaviour under blast loading: Part I — experimental investigation. International Journal of Impact Engineering, Vol. 90, 2016, pp. 1–13.
[4] LUCCIONI, B.M. - AMBROSINI, R.D. - DANESI, R.F.: Analysis of building collapse under blast loads. Engineering Structures, Vol. 26, Iss. 1, 2004, pp. 63–71.
[5] STEWART, M.G. - NETHERTON, M.D.: Blast load behaviour and design of composite steel–concrete members. Journal of Constructional Steel Research, Vol. 70, 2012, pp. 38–48.
[6] HAJEK, R. – FOGLAR, M. – VAVRIN, M. – HRADIL, P.: An experimental evaluation of the blast resistance of heterogeneous concrete-based composite bridge decks. Engineering Structures, Vol. 179, 2019, pp. 204–210, Elsevier BV.
[7] ZHAO, C. – LU, Y. – WU, C. – ZHANG, F. – TANG, Z.: Experimental and numerical investigation of steel–concrete (SC) slabs under contact blast loading. International Journal of Impact Engineering, Vol. 196, 2019, 109337, Elsevier BV.
[8] FOGLAR, M. – HAJEK, R. – KOVAR, M. – HRADIL, P.: Full-scale experimental testing of the blast resistance of HPFRC and UHPFRC bridge decks. Engineering Structures, Vol. 145, 2017, pp. 588–601, Elsevier BV.
[9] AOUDE, H. – DAGENAIS, M. – BURRELL, R. P. – SAATCIOGLU, M.: Behavior of ultra-high-performance fiber-reinforced concrete columns under blast loading. Journal of Structural Engineering, Vol. 141, Iss. 10, 2015, 04015028.
[10] RITCHIE, B. – REID, S. R. – SMITH, P. D. – CLARK, D.: Dynamic behaviour of concrete-filled rectangular hollow sections under blast loading. International Journal of Protective Structures, Vol. 9, Iss. 3, 2018, pp. 293–314.
[11] SAFAA, A. – KADHIM, M. M. A.: State of Research on Shear Strengthening / Repairing of RC Beams with Ultra-High-Performance Concrete (UHPC). *Civil and Environmental Engineering*, Vol. 0, No. 0, University of Žilina, 2025, https://doi.org/10.2478/cee-2025-0097.